Proceedings of CONF-FMCE 2026 Symposium: Artificial Intelligence and Smart Sensing for Mechanical and Electrical Systems
DOI: 10.54254/2755-2721/2026.BA36038

All-Carbon Interface Solar Steam Generator(ISSG)

Xinhe Bai

Shanghai Hongwen School, Shanghai, China
ttbai943@163.com

Abstract. Freshwater scarcity has driven growing interest in solar-driven desalination, among which interfacial solar steam generation (ISSG) offers a promising route by localizing photothermal conversion at the water–air interface to minimize heat loss. This review systematically examines the recent progress in all-wood-based ISSG devices, emphasizing the unique advantages of wood as a natural substrate—including its hierarchical porous architecture, intrinsic hydrophilicity, low thermal conductivity, and renewability. The composition and anisotropic structure of wood are first discussed in relation to water transport, capillary action, and thermal insulation. Subsequently, various photothermal coating materials—graphene, carbon nanotubes, carbon black, and ink—are compared in terms of preparation, efficiency, and cost, alongside matrix modifications such as delignification, carbonization, and nanocellulose-based porous structures. Key performance-limiting factors—sunlight absorption, heat loss (radiation, conduction, convection), absorber geometry, pore size, and environmental conditions (water depth, humidity, salinity)—are analyzed through quantitative formulas. Despite the eco-friendly and low-cost potential, practical scale-up faces challenges including high material costs, complex fabrication, salt crystallization, biofouling, and efficiency drops under weak illumination. The review concludes with future directions toward low-cost waste-derived photothermal layers, scalable processing, anti-salt structural design, and antifungal strategies, offering a comprehensive reference for sustainable ISSG development.

Keywords: Wood, Interfacial solar steam generation (ISSG), Photothermal materials, Wood structure, Thermal management

1. Introduction

Due to population growth and environmental pollution, fresh water resources on the earth are scarce, accounting for less than 3% of the world's water supply at present. Seawater desalination has become an important way to obtain fresh water, and it is very important to find an efficient method to produce fresh water. Solar steam generation is one of them.

Currently, there are two ways to generate steam using solar energy: Volumetric and Interfacial method.

The volumetric method can be understood as evaporating all the water in an entire area. Using this method can produce more fresh water, but it comes with some pretty serious downsides, like high costs, long time requirements, and heat loss. So, to overcome the many drawbacks mentioned

DOI: 10.54254/2755-2721/2026.BA36038

above, a method was designed that only evaporates the surface water in this area. In other words, photothermal conversion is limited to the water-air interface, so only the surface water gets heated, which is called the interfacial method.

ISSG mainly consists of two parts: the base and the photothermal coating. For the production of substrates, several materials with hydrophilic, porous, and insulating properties are now used as base materials. But using these kinds of polymer materials can make manufacturing too expensive, cause more environmental pollution, and worse, they could even be toxic to humans. For making photothermal coatings, people nowadays mostly use nanoparticles of silver and lead, as well as polymers and metals like graphene, but issues like high costs still remain. Wood has caught the attention of researchers because it's eco-friendly, highly sustainable, and low-cost, and its naturally abundant hydrophilic hydroxyl groups make it a possible candidate as an ISSG matrix. Also, wood-derived carbon materials have a broad absorption range and efficient photothermal conversion ability, making them ideal for photothermal coating materials.

This review will focus on showing the structures and physical-chemical properties of wood used in all-wood-based ISSG devices, as well as the materials used to make the devices. Finally, it sums up and looks ahead to future development directions. This review is expected to provide methods and approaches for the sustainable design and preparation of ISSG. This review aims to provide a systematic theoretical basis for the sustainable design and practical application preparation of ISSG equipment, so as to promote the implementation of solar steam technology in remote areas and resource-limited environments.

2. Wood structure and physical-chemical properties

2.1. Composition

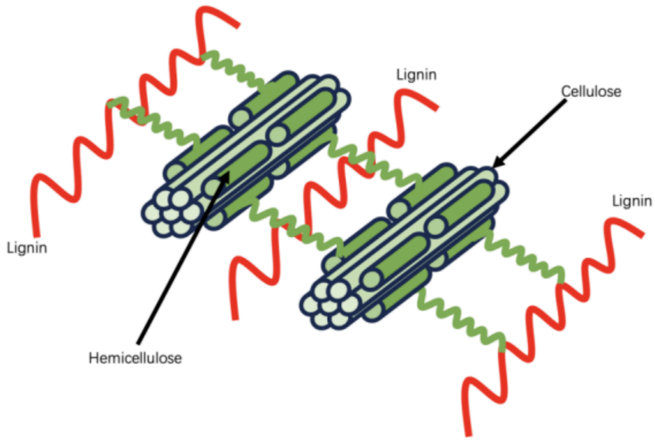

Figure 1. Composition of wood

As shown in Figure 1,wood is made up of cellulose (30-50% of the weight of the dry matter), hemicellulose (20-40% of the weight of the dry matter), and lignin (15-25% of the weight of the dry matter).

2.1.1. Cellulose

Cellulose is the primary structural material in plant cell walls. Its chemical composition is relatively uniform, mainly consisting of β-D-glucose and hemicellulose. In the cell wall, cellulose microfibrils

DOI: 10.54254/2755-2721/2026.BA36038

often intertwine with hemicellulose through hydrogen bonds and van der Waals forces, while also interacting with lignin to reinforce the cell wall, significantly boosting its mechanical strength and resistance to degradation.

2.1.2. Hemicellulose

Hemicellulose is a type of complex and highly branched heteropolysaccharide, usually made up of mannans, xylans, xyloglucans, β-glucans, and glucans. Hemicellulose and cellulose have a lot of highly hydrophilic groups, including hydroxyls, giving them great cell wall hydrophilicity and woody structure.

2.1.3. Lignin

Lignin is a type of phenolic polymer, made up of the polymerization of monolignols which help keep the stem strong and maintain the integrity of the cell structure.

2.2. Classification

Water movement in trees happens through the wood's porous structure, which is crucial for photosynthesis. Different types of wood also have different kinds of transport vessels.

2.2.1. Cork

Cork usually comes from coniferous trees. Common types of cork include cedar, pine, and yew, and because they grow quickly and are easy to get, they're pretty cheap. Its internal structure is honeycomb-like, with only sieve tubes, and it also has thin-walled tissues for transporting water. It has a low density, loose internal tissue, and thin cell walls.

2.2.2. Hardwood

Hardwood has a complex internal structure. It has both sieve tubes and vessels. The smaller sieve tubes support the woody structure, while the larger vessels help with water transport. It has a higher density, a more compact internal structure, and thicker cell walls. Hardwood typically comes from broad-leaved trees, and its seeds are contained in fruits or pods. Because it has a longer growth cycle, is harder to get, and requires more complex processing, it's more expensive than cork. In the ISSG, compared to cork, hardwood's more open and connected pore system helps water move through it better.

2.3. Properties

2.3.1. Anisotropy

Anisotropic structures include longitudinal, radial, and chordwise directions.

The longitudinal direction is parallel to the trunk (the way the tree grows). Wood cells (fibers, vessels, tracheids) are mainly arranged along this direction. This direction has the highest strength, and water and liquids can most easily penetrate and flow along it.

The radial direction is perpendicular to the trunk and passes through the center of the pith (that is, along the wood rays). It has moderate strength and is the main pathway for lateral water conduction.

DOI: 10.54254/2755-2721/2026.BA36038

The grain runs in a direction perpendicular to the trunk but tangent to the wood rays (that is, parallel to the growth ring lines). The strength in this direction is usually the lowest.

2.3.2. Thermal conductivity

When there's a temperature difference inside a material (a temperature gradient), heat flows from the hotter area to the cooler area.

As a natural thermal insulator, wood has very low thermal conductivity, which makes it one of the candidates for an insulating substrate in efficient interfacial solar steam generation. At the same time, because of its anisotropic structure, wood conducts heat differently in different directions.

2.3.3. Density and porosity

Porosity refers to the percentage of the internal pore volume of a material relative to its total volume. It shows how loose the internal structure of a material is, or how much liquid it can hold. Density and porosity can change the performance of wood in the application of interfacial solar steam power generation. Porosity is an important characteristic of wood, which can affect the efficiency of solar steam generation at the interface. The rough surface of wood has a large area to support a large amount of light absorption.

2.3.4. Capillary action

Capillary action is when a liquid moves on its own in narrow spaces, like the cell cavities or pits in wood, using surface tension and wettability, either overcoming or taking advantage of gravity. Due to the cohesion of water molecules and the capillary action of wood, water can move from the bottom to the top of the wood.

3. Preparation of wood-based ISSG

3.1. Photothermal material

Solar thermal materials are responsible for turning solar radiation into heat, and they are the key factor that determines the overall energy conversion efficiency of the system. At present, researchers have developed various photothermal material systems, mainly including graphene, carbon nanotubes, carbon black, ink, and so on.

3.1.1. Graphene

Many people have used graphene oxide reduction as a coating. This method requires chemical preparation and is relatively complicated. Its advantage is excellent thermal conductivity, with photo-thermal conversion efficiency reaching 86%-98%. But the downside is that it's extremely expensive.

Liu and others used the porous capillary action of wood to create a hollows structure of holly leaf-like graphene (HLG), boosting light absorption, with a thermal conductivity of only 0.074 W/(m·K), achieving efficient localized heating. The evaporation rate under 1 sun is 1.96 $kg \cdot m^{-2} \cdot h^{-1}$, with an energy conversion efficiency as high as 94.2% [1].

Bang and others built a bionic transpiration double-layer structure (hydrophilic C-WOOD bottom layer pumps water / hydrophobic rGO top layer evaporates), with 3D micro reservoirs between

DOI: 10.54254/2755-2721/2026.BA36038

layers reducing heat loss. Under 1 sun illumination, the evaporation rate is 1.492 $kg \cdot m^{-2} \cdot h^{-1}$ with an efficiency of 94.7%, and it stays stable over cycles [2].

3.1.2. Carbon nanotubes

Carbon nanotubes have a high aspect ratio, making it easier to create 3D structures on surfaces to boost sunlight absorption, but dispersion and coating processes can be tricky, so surface modification is often needed. Its photothermal conversion efficiency is greater than or equal to 80%. Its advantage is that the porous structure helps steam escape. The downside is that it tends to clump together, is hard to disperse, and as a pure blackbody, it has poor spectral selectivity.

Ge-Zhang and others coated a mixture of MWCNTs and carbon black onto delignified wood, forming a rough, cross-linked coating with a broadband absorption of about 97.5%. This structure achieved an evaporation efficiency of 51.1% within 24 hours, outperforming natural or purely delignified wood devices [3].

Li and his colleagues used the one-step combustion method to apply Fe_2O_3/CNT to the surface of wood, enabling efficient photothermal conversion; the vertical channels in the wood helped to concentrate heat on the coating. Under 1 sun, the evaporation rate was 1.42 $kg \cdot m^{-2} \cdot h^{-1}$, with an efficiency of 87.2% [4].

3.1.3. Carbon black

This method has the simplest preparation process and can be done by spraying or dipping, making it easy for large-scale production. It's also suitable as a supplement to CNTs, adding nanoscale effects. Its photothermal conversion efficiency is moderate, but can reach up to 98% when mixed with other materials. The advantage is that it's super low-cost. The downside is that pure carbon black coatings don't handle water well and have relatively poor mechanical stability.

Researchers pointed out in their research on new wood-based photothermal materials that black coatings like carbon black tend to fall off easily because they don't stick well to the substrate. Even though they didn't use it as the main coating, it was used for comparison to highlight the limitations of traditional carbon black coatings [5].

3.1.4. Ink

The outstanding advantage of this method is that its operating threshold is extremely low-it is not necessary to design or synthesize any photothermal conversion materials by itself, and it can be put into application by directly using the commercially available or ready-made formula system, which truly realizes the convenience of "ready to use". However, its photothermal conversion performance is not constant, but highly depends on the specific components and proportion of the formula adopted, and the efficiency difference between different commercial products or customized slurries may be significant; Generally speaking, the energy conversion level of this kind of system is mostly in the middle range, which is not comparable to the extreme optimization results of frontier laboratories, but also enough to meet the basic needs of most conventional scenarios.

Zhang and others used waste printer toner (mainly composed of carbon black and iron oxide) combined with delignified balsa wood to create a Janus-structured evaporation interface. Under 1 sun of light intensity, it achieved an evaporation rate of 1.79 $kg \cdot m^{-2} \cdot h^{-1}$ and a photothermal conversion efficiency of 94.1%, with excellent salt resistance and stability [6].

DOI: 10.54254/2755-2721/2026.BA36038

Tariq and others combined pencil graphite (a carbon-based material) with cellulose paper, and under three times the intensity of sunlight, the evaporation rate reached 4.32 $kg \cdot m^{-2} \cdot h^{-1}$, about 3.5 times that of the untreated membrane, offering an idea for a solvent-free, fast way to make photothermal layers [7].

3.2. Matrix

3.2.1. Direct use of natural wood

Wood doesn't need much processing, and it's cheap and eco-friendly. But soaking in water for a long time can make wood rot, which is definitely a cost-increasing drawback.

Li and others used adjustable vapor deposition to grow polythiophene nanowires/button-like structures in situ on the surface of spruce veneer (0.6 mm thick) with a reverse tree structure. Under 1 sun, the evaporation flux was 1.48 $kg \cdot m^{-2} \cdot h^{-1}$, and the photothermal efficiency is 92.4% [8].

Liu and others used waste polyester to control carbonization and create low-cost porous carbon (with oxygen functional groups and micro/meso/macropores), which they coated on wood surfaces. The coating enhances light absorption and promotes water clustering to reduce evaporation enthalpy. Under 1 sun illumination, the evaporation rate reached 2.38 $kg \cdot m^{-2} \cdot h^{-1}$, and it remained stable and salt-resistant [9].

3.2.2. Delignification and modification

The delignification process boosts the wood's ability to conduct water and reduces its heat conductivity and heat loss.

Ma and colleagues soaked delignified balsa wood in sodium alginate hydrogel, then in situ polymerized and modified it with flaky PPy. Under 1 sun, the evaporation rate was 2.03 $kg \cdot m^{-2} \cdot h^{-1}$, the photothermal efficiency was 92.4%, and it was salt-resistant and anti-fouling [10].

Tian and others expanded the pores by removing lignin and hemicellulose, then grafted sulfonic acid groups to weaken the hydrogen bonds of water molecules. After optimization, the wood's water absorption reached 6.5 $g \cdot g^{-1}$, and its evaporation enthalpy dropped to 1197 $J \cdot g^{-1}$. Under one sun of sunlight, the evaporation rate reached as high as 3.4 $kg \cdot m^{-2} \cdot h^{-1}$, with a photothermal efficiency of 97.2% [11].

3.2.3. Carbonization

Carbonized mesoporous wood, which features long-term stability and resistance to contamination, can absorb 99% of solar energy and generate efficient interfacial solar steam.

Luo and others carbonized the surface of poplar to get SCW, then deposited Ag nanoparticles and $MgFe_2O_4$ in situ to build a sandwich-structured dual-function reactor. Under one sun of light, the evaporation rate was 1.55 $kg \cdot m^{-2} \cdot h^{-1}$ with an efficiency of 88.6%, and it maintained stable long-term performance in simulated wastewater as well as in strong acidic and alkaline solutions [12].

Yang and others carbonized pretreated balsa wood, then deposited a polydopamine (PDA) hydrophilic coating using dopamine (DA) and diethylenetriamine (DETA), creating superhydrophilic carbonized wood (SCW). Under 1 sun of light: the net evaporation rate of seawater was 1.7853 $kg \cdot m^{-2} \cdot h^{-1}$ with an efficiency of 91.81%, and 1.52538 $kg \cdot m^{-2} \cdot h^{-1}$ of 78.44% [13].

DOI: 10.54254/2755-2721/2026.BA36038

3.2.4. Porous materials made from nanocellulose

Tian and others used TOCNFs as raw materials, and through freeze-thaw embedding, Fe^{3+} complex-directed stabilization, and ambient pressure drying, they prepared ordered porous NCA. They then coated it with PPy to get a composite material with both photothermal properties and continuous channels, which is used for efficient solar evaporation [14].

Lin and others used a cellulose-based hydrogel (LCG) as the matrix and lignin-derived carbon (LC) as the photothermal material to create a fully cellulose-based bilayer hydrogel evaporator. The lignin boosts hydrophilicity, maintains capillary channels, and regulates water in an intermediate state to lower the heat of vaporization while ensuring a high rate of water transporting. Under 1 sun of sunlight, the evaporation rate is 1.84 $kg \cdot m^{-2} \cdot h^{-1}$ with an efficiency of 86.5% [15].

4. Influencing factors

4.1. Sunlight absorption

The materials, microstructures, and spectral response characteristics of the light-absorbing coating determine the efficiency with which the device converts solar radiation into thermal energy.

4.2. Heat loss

An ideal photothermal evaporator should localize heat at the evaporation interface, but in reality, heat loss often occurs. Therefore, effectively reducing heat loss caused by radiation, conduction, and convection is central to improving evaporation efficiency. The main modes of heat loss include radiation, conduction, and convection.

4.2.1. radiation

Radiation loss can be quantified by the Stefan–Boltzmann equation (Eq. 1):

$$Prad = \epsilon \sigma A\left(T_s^4 - T_{amb}^4\right) \tag{1}$$

ϵ is the surface emissivity, σ is the Stefan–Boltzmann constant, A is the surface area, $\boldsymbol{T_s}$ is the evaporation surface temperature, and $\boldsymbol{T_{amb}}$ is the ambient temperature. Using an absorption coating with low infrared emissivity can effectively reduce radiation loss.

4.2.2. Conduction

Heat loss mainly includes thermal conduction from the solid substrate to the water body and the surrounding environment. The conductive heat loss is given by Eq. (2), while the thermal resistance is defined by Eq. (3):

$$\varphi = Mc\Delta T \tag{2}$$

φ is the conductive heat loss, c is the specific heat capacity of pure water. M is the weight of the water, and ΔT is the temperature change after the water evaporates.

Thermal resistance:

DOI: 10.54254/2755-2721/2026.BA36038

$$\Omega = \mathrm{v}/\mathrm{TC} \times \mathrm{A} \tag{3}$$

Ω is the thermal resistance, and v is the thickness of the wooden solar steam power device. TC stands for thermal conductivity.

So, using wood with low thermal conductivity as the base and optimizing its thickness is an effective way to prevent heat from escaping into the water.

4.2.3. Convection

Heat loss primarily originates from the thermal exchange between the evaporative surface and the air. Convective heat loss follows Newton's law of cooling, as expressed in Eq. (4):

$$\Lambda = \mathrm{HA}\Delta\mathrm{T} \tag{4}$$

Λ is the heat transfer rate. H is the convective heat transfer coefficient. A is the surface area of the light absorber.

4.3. Geometric shapes of light absorber

The evaporation efficiency of the light-absorbing part heavily depends on its shape. Optimizing the shape (like building 3D structures or increasing surface roughness) can boost multiple internal reflections and light absorption, expand the evaporation area, and adjust how heat is distributed and transferred. 3D structures can also trigger extra water transport and air convection effects. Its thermal efficiency η_1 and conductive heat loss φ can be quantitatively analyzed using the following formulas:

The thermal efficiency η_1 of the light absorber is calculated by Eq. (5):

$$\eta_1 = \left(\propto - \frac{\boldsymbol{\varepsilon\Pi}(\boldsymbol{T}_1^4 - \boldsymbol{T}_0^4)}{\boldsymbol{q_s}} - \frac{\boldsymbol{H}(\boldsymbol{T}_1 - \boldsymbol{T}_0)}{\boldsymbol{q_s}} - \frac{\boldsymbol{\varphi}}{\boldsymbol{q_s}}\right) \times 100\% \tag{5}$$

H is the convective heat transfer coefficient. φ is the conductive heat loss of the solar absorber. $\boldsymbol{q_s}$ is the solar irradiance, Π is the Stefan-Boltzmann constant, ε is the emissivity of the solar absorber surface, $\boldsymbol{T}_0$ is the initial temperature of the surrounding environment, and $\boldsymbol{T}_1$ is the final temperature of the solar absorber surface after irradiation.

The conductive heat loss φ of the light absorber is determined by Eq. (6):

$$\varphi = \frac{(\boldsymbol{T}_1 - \boldsymbol{T}_0)}{\frac{\boldsymbol{v}}{\boldsymbol{TC_p}} + \frac{\boldsymbol{Z}_0}{\boldsymbol{TC_w}}} \tag{6}$$

v is the thickness of the light absorber, $\boldsymbol{TC_p}$ is the thermal conductivity of the light absorber, $\boldsymbol{Z}_0$ is the distance between the bottom of the container and the bottom of the light absorber, and $\boldsymbol{TC_w}$ is the thermal conductivity of water.

The maximum efficiency of water transmission η_2 is obtained from Eq. (7):

$$\eta_2 = \frac{\boldsymbol{h_{Lv}}\dot{\mathrm{m}}_{\boldsymbol{f}}}{\boldsymbol{q_s}} \times 100\% \tag{7}$$

$\dot{\mathrm{m}}_{\boldsymbol{f}}$ is the evaporation flux. $\boldsymbol{h_{Lv}}$ represents the total enthalpy of evaporation of water. $\boldsymbol{q_s}$ is solar radiation.

DOI: 10.54254/2755-2721/2026.BA36038

The water flow rate for evaporators of different thicknesses is given by Eq. (8):

$$\dot{m}_f = \frac{\rho\sigma\varphi d}{4\tau\mu v} \tag{8}$$

ρ is the density of water. φ is the porosity of the wood. σ represents the surface tension of water, d is the diameter of the microchannel, and μ is the fluid viscosity. τ is the tortuosity of the microchannels in the light absorber. v is the thickness of the light absorber.

4.4. Aperture

The pore size of a wooden solar steam generator affects the evaporation enthalpy. So, a wood substrate with suitable nanopores can lower the energy needed for evaporation and boost efficiency.

Enthalpy $\boldsymbol{H}$ is defined by Eq. (9):

$$\boldsymbol{H} = \boldsymbol{E} + \boldsymbol{PV} \tag{9}$$

E is the internal energy. V represents volume, and P represents pressure. Thus, the gas-phase enthalpy $\boldsymbol{E_g}$ and liquid-phase enthalpy $\boldsymbol{E_l}$ are expressed by Eqs. (10) and (11), respectively:

$$\boldsymbol{H_g} = \boldsymbol{E_g} + \boldsymbol{P_g V_g} \tag{10}$$

$$\boldsymbol{H_l} = \boldsymbol{E_l} + \boldsymbol{P_l V_l} \tag{11}$$

$\boldsymbol{P_g}$, $\boldsymbol{V_g}$, $\boldsymbol{P_l}$ and $\boldsymbol{V_l}$ are the pressure and volume of the gas and liquid phases.

4.5. Environmental conditions

4.5.1. Water depth

The device draws water to the evaporation surface through capillary action, and it can maintain the right height difference between the irradiated surface and the water level.

4.5.2. Relative humidity

The relative humidity of the environment might not be an accurate indicator of the actual moisture level in wooden solar steam power equipment. The results show that even at high environmental relative humidity, the evaporation rate doesn't drop significantly under sunlight. Temperature plays a key role in evaporation efficiency, so it should be considered in heat loss calculations rather than just the ambient temperature.

4.5.3. Water salinity

High salt levels (like in seawater or concentrated brine) can really affect how well an all-wood solar steam generator evaporates water. Salt can crystallize on the evaporation surface and clog the natural tiny channels in the wood, which blocks water flow. At the same time, the salt crystals can reflect and scatter sunlight, lowering the efficiency of converting sunlight into heat and slowing down the evaporation rate. So, making all-wood evaporators that can handle salt well is key to making them practical.

DOI: 10.54254/2755-2721/2026.BA36038

5. Conclusion

This article reviews the research progress of all-wood-based interface solar steam generation (ISSG) devices. It first highlights the unique advantages of wood as a substrate, including its hierarchical porous structure, good hydrophilicity, low thermal conductivity, and natural renewability. Then, it systematically goes over the selection principles of various photothermal materials used as substrates for ISSG.

Although all-wood-based ISSG devices have attracted attention for being environmentally friendly and using cheap raw materials, they still face scalability and cost-effectiveness bottlenecks in practical large-scale applications. Specifically, they mainly face the following five challenges:

High-cost challenges and the development of low-cost photothermal materials: The high price of high-performance photothermal materials (like noble metal nanoparticles) is a major barrier to their large-scale use. Researchers should shift towards using waste biomass to develop low-cost alternatives.

Innovation in complex preparation processes and simple, scalable methods: The manufacture of many devices involves multiple chemical treatments or precise coatings, making large-scale production difficult. Researchers should develop simple, scalable modification methods.

Dependence on strong lighting and building broadband high-efficiency light-absorbing coatings: device performance is usually best under strong light and drops under low-light conditions. To reduce dependence on constant high-intensity light, researchers are working on creating broadband high-efficiency light-absorbing coatings.

Salt buildup blockage and the design of adjustable island structures: During evaporation, salt crystallizes on surfaces or within pores, blocking water channels and reducing light absorption. Researchers have proposed effective structural design ideas to address the issue of salt blockage.

Bio-contamination and mold prevention issues, and the application of 3D antifungal structures: Wood used for long periods in humid, salty environments is prone to microbial and mold growth, leading to structural damage and performance decline. Researchers should focus on giving materials inherent antifungal properties to enhance their durability in harsh water environments.

This article can help with the theoretical study, material selection, and problem-solving for fully wood-based ISSG devices.

References

[1] Liu, S., et al. (2024). Micronleaf-shape graphene interfaces on wood transverse sections as advanced photothermal evaporators for water purification. *Journal of Materials Science & Technology, 193*, 81-89.

[2] Bang, J., Moon, I. K., & Oh, J. (2023). Three-dimensional multimodal porous graphene-carbonized wood for highly efficient solar steam generation. *Sustainable Energy Technologies and Assessments, 57*, 103199.

[3] Ge-Zhang, S., Tang, G., Yang, H., & Mu, H. (2023). Interfacial solar steam generator by MWCNTs/carbon black nanoparticles coated wood. *Alexandria Engineering Journal, 63*, 1-10.

[4] Li, W., Li, X., Liu, J., Zeng, M. J., Feng, X., Jia, X., & Yu, Z. Z. (2021). Coating of wood with Fe_2O_3-decorated carbon nanotubes by one-step combustion for efficient solar steam generation. *ACS Applied Materials & Interfaces, 13*(19), 22845–22854.

[5] He, F., Han, M., Zhang, J., Wang, Z., Wu, X., Zhou, Y., ... & Li, Y. (2020). A simple, mild and versatile method for preparation of photothermal woods toward highly efficient solar steam generation. *Nano Energy, 71*, 104650.

[6] Zhang, W., Liu, S., Liu, J., Huang, E., Wang, R., Zuo, Q., & Gong, L. (2024). Turning waste into treasure: Utilizing discarded printer toner-modified wood for efficient solar water evaporation in diverse water environments. *Separation and Purification Technology, 354*, 128907.

[7] Tariq, M. Z., Hanif, Z., La, M., Choi, D., & Park, S. J. (2021). Pencil-traced-graphite on cellulose: A rapid and solvent-less approach for solar steam generation. *International Journal of Energy Research, 45*(4), 6395-6404.

DOI: 10.54254/2755-2721/2026.BA36038

[8] Li, M., Sun, Y., Lei, Y., Liu, G., Jiang, H., Wang, Y., ... & Hu, J. (2024). Nature-inspired ultrathin wood-based interfacial solar steam generators for high-efficiency water purification. *Desalination, 587*, 118018.

[9] Liu, N., Hao, L., Zhang, B., Niu, R., Gong, J., & Tang, T. (2021). Rational design of high-performance bilayer solar evaporator by using waste polyester-derived porous carbon-coated wood. *Energy & Environmental Materials, 5*(2), 617-626.

[10] Ma, W., Nie, Y., Cao, W., Fan, Q., Wen, J., Zhang, Y., ... & Gong, X. (2025). Bioinspired, robust wood solar evaporator with scale-like surfaces for efficient solar-driven water purification and thermoelectric generation. *Chemical Engineering Journal*, 159286.

[11] Tian, M., Xie, Y., Lv, M., ... et al. (2025). Natural wood with optimal capillary water content and evaporation enthalpy for efficient interfacial solar steam generation. *Materials Horizons*. DOI: 10.1039/D5MH00394F.

[12] Luo, S., Liu, Z., Yin, X., Lin, Z., Zhang, S., Chen, J., & Guo, M. (2024). A sandwich structure Ag/MgFe2O4-deposited surface carbonized wood for integrated solar steam generation and photoreduction of Cr (VI). *Small*.

[13] Yang, Y., Wang, H., Sun, Q., & Li, Y. (2024). Super-hydrophilic carbonized wood-based solar steam evaporator: A novel approach to enhance freshwater generation. *Journal of Industrial and Engineering Chemistry*.

[14] Tian, J., Huang, Y., Zhang, X., Wang, J., Fei, B., & Wu, W. (2022). Anisotropic cellulose nanofibril aerogels fabricated by directional stabilization and ambient drying for efficient solar evaporation. *Chemical Engineering Journal, 450*, 138191.

[15] Lin, X., Wang, P., Hong, R., Zhu, X., Liu, Y., Pan, X., Qiu, X., & Qin, Y. (2022). Fully lignocellulosic biomass-based double-layered porous hydrogel for efficient solar steam generation. *Advanced Functional Materials, 33*(3), 2209262.